Supplementary Material for:

Interface and layer periodicity effects on the thermal conductivity of copper-based nanomultilayers with tungsten, tantalum, and tantalum nitride diffusion barriers

Claudia Cancellieri,[1, a)] Ethan A. Scott,[2, a)] Jeffrey Braun,[2] Sean W. King,[3] Ron Oviedo,[3] Christopher Jezewski,[3] John Richards,[3] Fabio La Mattina,[1] Lars P.H. Jeurgens,[1] and Patrick E. Hopkins[2, 4, 5, b)]

[1)]*Empa, Swiss Federal Laboratories for Materials Science and Technology, Überlandstrasse 129, 8600 Dübendorf, Switzerland.*

[2)]*Department of Mechanical and Aerospace Engineering, University of Virginia, Charlottesville, VA 22904*

[3)]*Logic Technology Development, Intel Corporation, Hillsboro, Oregon 97124, USA*

[4)]*Department of Materials Science and Engineering, University of Virginia, Charlottesville, VA 22904*

[5)]*Physics Department, University of Virginia, Charlottesville, VA 22904*

[a)]Claudia Cancellieri and Ethan A. Scott contributed equally to this work

[b)]Electronic mail: phopkins@virginia.edu

CONTENTS

I. XRD ON SINGLE LAYERS

Select reference samples of single layers of Ta and of Cu have been fabricated and measured. In Fig.S1 a), the XRD patterns of pure Ta layer of 100 nm thickness deposited on Cu300nm/Si substrate is reported. Apart from the peaks of the underneath Cu layer, the Ta layer appears to be in the beta-phase and preferentially oriented along the [001] direction. The Cu buffer layer, in Fig.S1 b), shows polycrystallinity due to the presence of different reflections and as well as some oxidation due to air exposure.

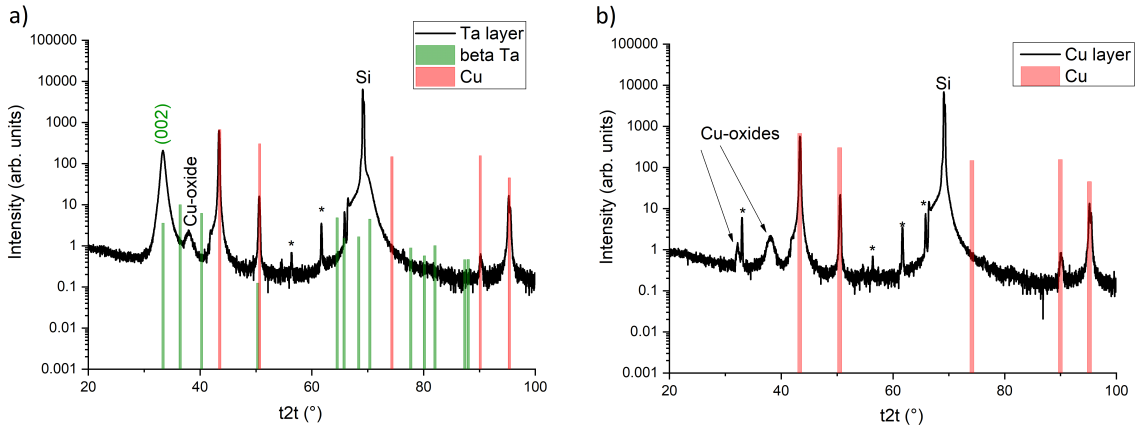

FIG. S1. XRD diffraction of the a) 100nm Ta layer deposited on Cu (300nm) buffer on S and of b) blank Cu buffer layer. The peaks labelled with asterisks indicate spurious reflections due to non-monochromatic radiations (k_β, tungsten)

.

II. AFM

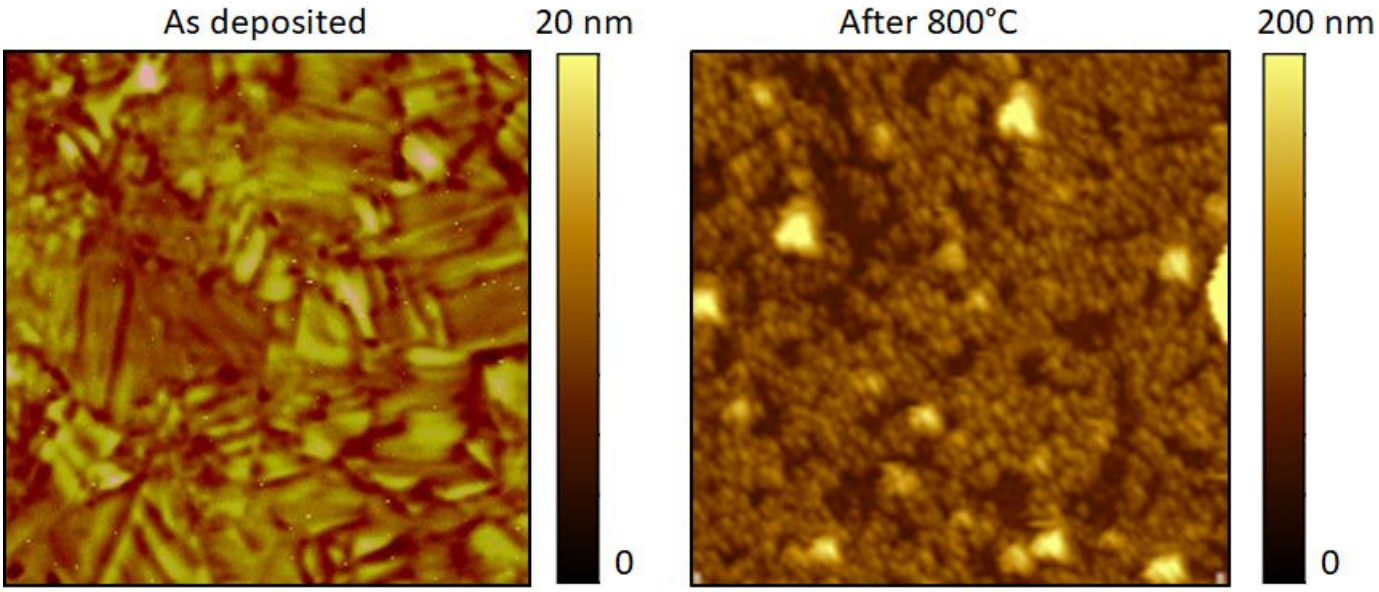

FIG. S2. AFM images for the Cu 5nm/Ta5nm x 11 sample before and after annealing at 800°C. Note the different vertical scales.

The average surface roughness derived by AFM in a 5 x 5 μm^2 area is always around or less than 2 nm for all the as deposited samples. After 800°C annealing, the average surface roughness in the same area is around 70-80 nm.

III. SHEET RESISTANCE MEASUREMENTS

Sheet resistance measurements were performed on select samples at room temperature by using a 4-probe resistance setup composed of four equally spaced tungsten metal tips with finite radius. Each tip is supported by springs on the other end to minimize sample damage during probing. In this configuration, sheet resistance (R_s) is measured and if the thickness (t) of the conducting layer is known, the resistivity can be obtained. The sheet resistance for Cu thin films was converted to resistivity, ρ ($\rho = R_s t$), for each known thickness as shown in Figure S3:

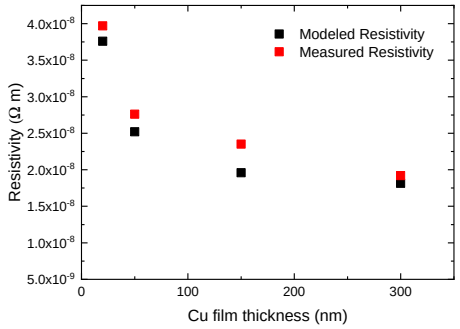

FIG. S3. Resistivity of Cu films

For 300 nm Cu films we find R_s = 69 m$\Omega\square^{-1}$ which corresponds to ρ= 2.07×10^{-8} Ω m. The obtained value is similar to the nominal bulk value for Cu found in literature. The observed trend with Cu thickness indicates an expected size effect that can be modeled considering the contribution of grain boundary scattering introduced by Mayadas *et al.*[1] for a metal thin film with columnar grains with an average lateral grain size (D).[2] For W, we measured a 300 nm layer and find R_s= 300 m$\Omega\square^{-1}$ and ρ= 9×10^{-8} Ω m, also in line with the nominal bulk value.

We note that the measured electrical resistance from four-point-probe is in-plane, due to the geometry, while the thermal conductivity measurements from TDTR presented in the paper are out-of-plane. An out-of-plane measurement would require a proper contact design, including a bottom electrode with specific dimensions, which was not be fabricated for this sample set. We find the sheet resistance measured for each Cu/Ta(N) sample in the as deposited state to fall between 62 and 67 mΩ m, which is indicated by the gray region of Figure S4.

As all multilayer samples are fabricated upon a 300 nm Cu layer, there is potential for convolution of the resultant measured electrical resistance. However, a significant change is observed in the case of high temperature annealing (800 °C). When the multilayer systems degrade into nanocomposites, a significant increase in resistance is observed. This is in contrast to the ther-

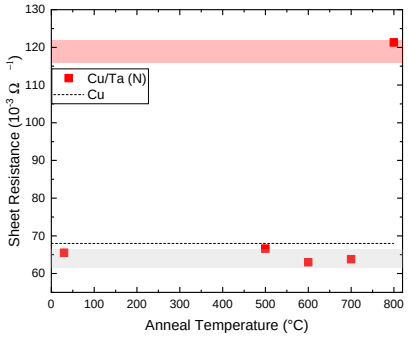

FIG. S4. Sheet resistance measured for the Cu/Ta(N) multilayers before and after annealing. The gray region indicates the window of values found for all the multilayers in the as-deposited state while the red region indicates the window of values found for the multilayers, independently of their thickness, after annealing. The points displayed are for a representative sample, Cu 5nm/Ta 5nm x 11.

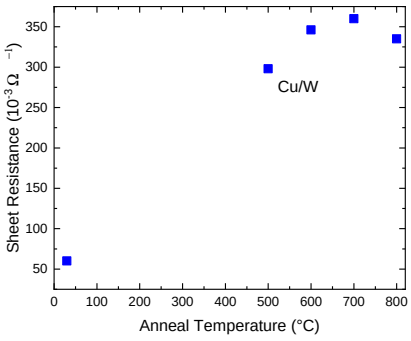

FIG. S5. Sheet resistance measured for the Cu/W multilayers as a function of anneal temperature. The points displayed are for a representative sample, Cu 5nm/W 5nm x 100.

mal conductivity measurements in which large increases in thermal conductivity are observed. However, this finding serves to enforce the veracity that the two measurements are fundamentally different: in the case of nanocomposite formation, scattering sources are formed in an otherwise pristine layer, which reduces the in-plane conductivity measured through four-point probe measurement. In contrast, the loss of distinct layers in the cross-plane direction reduces carrier scattering, yielding a higher thermal conductivity in the cross-plane direction, observed in TDTR measurement.

In addition, sheet resistance measurements were performed on a Cu/W 5 nm/5 nm x 100 sample, in the as-deposited state as well as after annealing, shown in Figure S5. Analogously to

Cu/Ta(N), the sheet resistance increases upon annealing, but with an onset beginning at lower temperatures. The Cu/W system decomposes gradually by thermal annealing starting at T $\geq$ 500 °C and the degradation process continues up to 800 °C where a complete multi-layer-to-nanocomposite transition is achieved.[3,4]

IV. THERMAL MEASUREMENT SENSITIVITIES

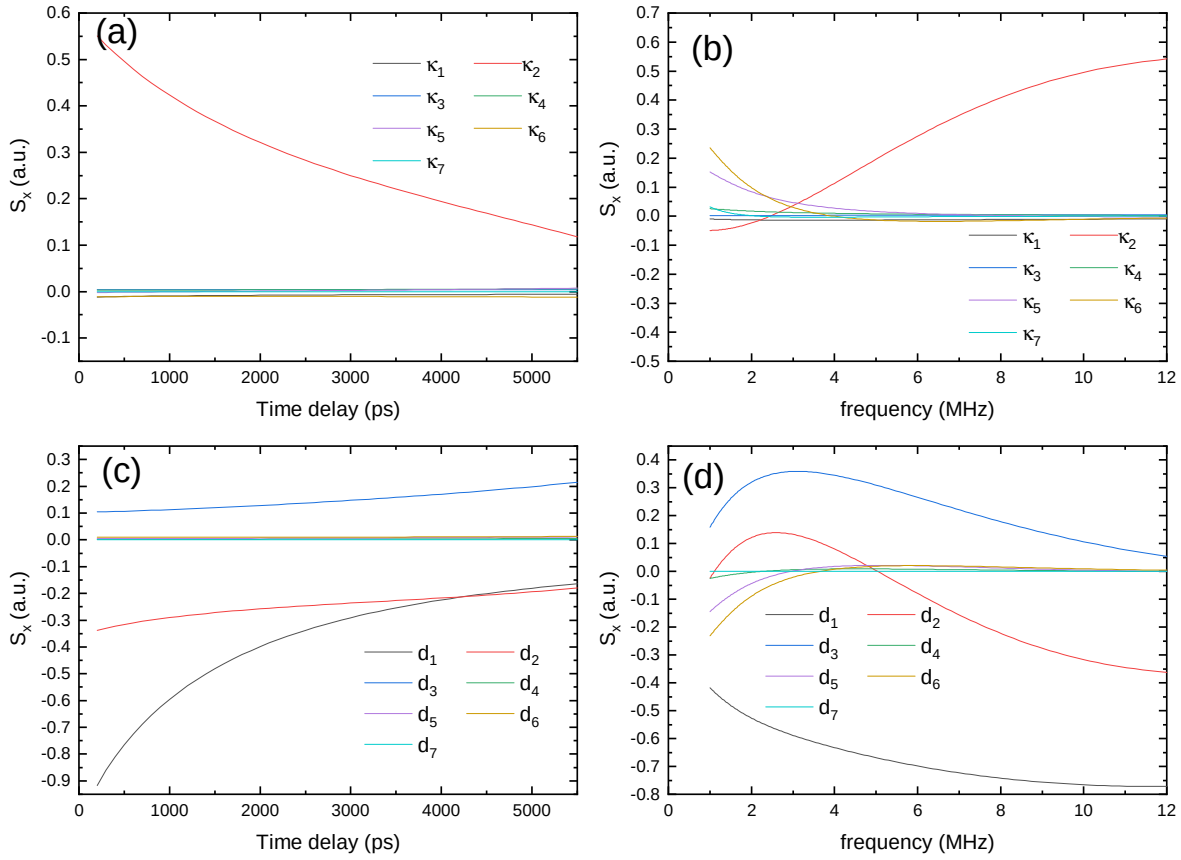

FIG. S6. Example parameter sensitivity calculations for the Cu/Ta, Cu/TaN samples. The sensitivity, S_x, to a given parameter, x, is calculated in the method laid out by Gundrum et. al[5] as both a function of time (a,c) and frequency (b,d). The parameters of the thermal model are tabulated in Table S1. The sensitivity of the thermal model is calculated for parameters including the thermal conductivity, κ, of each layer, as well sensitivity to layer thickness, d. In the thermal model, the thermal conductivity of the multilayer region, κ_2, and the thermal boundary conductance between the aluminum capping layer and metal multilayer region, G_1, are used as fitting parameters. It can be seen from the sensitivity analysis that there is high sensitivity to the metal multilayer region as it is one of the most thermally resistive regions. Furthermore, sensitivity to the region increases at higher frequencies. As such, TDTR measurements are performed at 10 MHz.

TABLE S1. Material properties used for the Cu/Ta, Cu/TaN sensitivity analysis (Figure S6). For both material systems, a seven layer model is applied, along with pump and probe diameters of 33 and 14 μm, respectively. The thermal conductivity of the multilayer region, κ_2, and the thermal boundary conductance, G_1, between the aluminum capping layer and the multilayer region are used as fit parameters in the thermal model. In the example shown, the fitted thermal conductivity and thermal boundary conductance were found to be 8.82 W m^{-1} K^{-1}and 121 MW m^{-2} K^{-1}, respectively. The heat capacity of the multilayer region is calculated by applying a rule of mixtures formulation to the constituent heat capacities. In a previous study,[6] it was demonstrated that in dielectrics and oxides greater than 10 nm, the bulk of the thermal resistance is intrinsic to the film as opposed the interfacial resistances, and therefore we approximate the intrinsic thermal resistance of the other films to be much higher than their associated interfacial resistance, and set the associated thermal boundary conductances as infinite. The thicknesses of the multilayer region, Cu buffer layer, and Ta(N) buffer layer are measured with cross sectional scanning electron microscopy (XSEM). Other parameters such as heat capacity of the films, C_v are taken from literature.

System	Layer	Material	d (nm)	C_v (MJ m^{-3} K^{-1})	κ (W m^{-1} K^{-1})
Cu/Ta(N)					
	1	Al	80	2.43[7–9]	135[9,10]
	2	Cu/Ta(N)	238	2.89	8.82
	3	Cu	268.1	3.45[11]	398[12,13]
	4	TaN	28.59	2.18[14]	3[15]
	5	SiN	100	2.1[16]	2.1[17,18]
	6	SiO_2	100	1.65[9]	1.35[9,18]
	7	Si	bulk	1.65[9]	140[19]

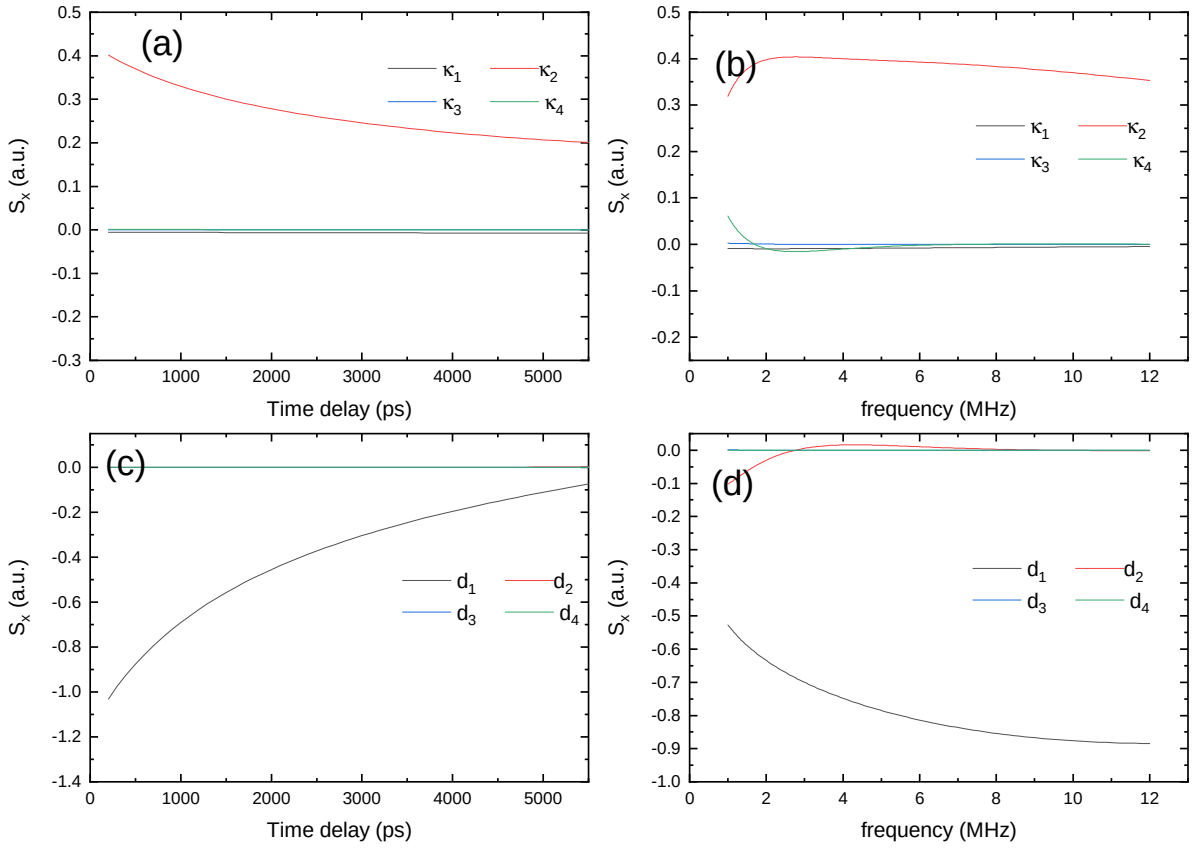

FIG. S7. Example parameter sensitivity calculations representative of the Cu/W samples. The sensitivity is calculated in the same way as in the Cu/Ta(N) case, but assuming a four layer model, the parameters of which are laid out in Table S2. Similar to Figure S6, (a) and (c) display the measurement sensitivity as a function of delay time to the film thermal conductivities and thicknesses, whereas (b) and (d) display this information as a function of modulation frequency.

TABLE S2. Material properties used for the Cu/W sensitivity analysis (Figure S7). A four-layer model is applied, along with pump and probe diameters of 33 and 14 μm, respectively. The thermal conductivity of the multilayer region, κ_2, and the thermal boundary conductance, G_1, between the aluminum capping layer and the multilayer region are used as fit parameters in the thermal model. In the example shown, the fitted thermal conductivity and thermal boundary conductance were found to be 19.8 W m^{-1} K^{-1}and 68.9 MW m^{-2} K^{-1}, respectively. The thermal boundary conductance between the other regions is treated as infinite as described in Table S1. Furthermore, as in the previous example, the heat capacity of the multilayer region is calculated by applying a rule of mixtures formulation to the heat capacity values of the constituent layers. Other properties are taken from literature, and cited accordingly.

System	Layer	Material	d (nm)	C_v (MJ m^{-3} K^{-1})	κ (W m^{-1} K^{-1})
Cu/W					
	1	Al	80	2.43[7–9]	135[9,10]
	2	Cu/W	1300	3.25	19.8
	3	W	25	2.56[20]	52.2[21]
	4	Al_2O_3	bulk	3.02[7]	35[19]

V. CU, W THERMAL CONDUCTIVITIES

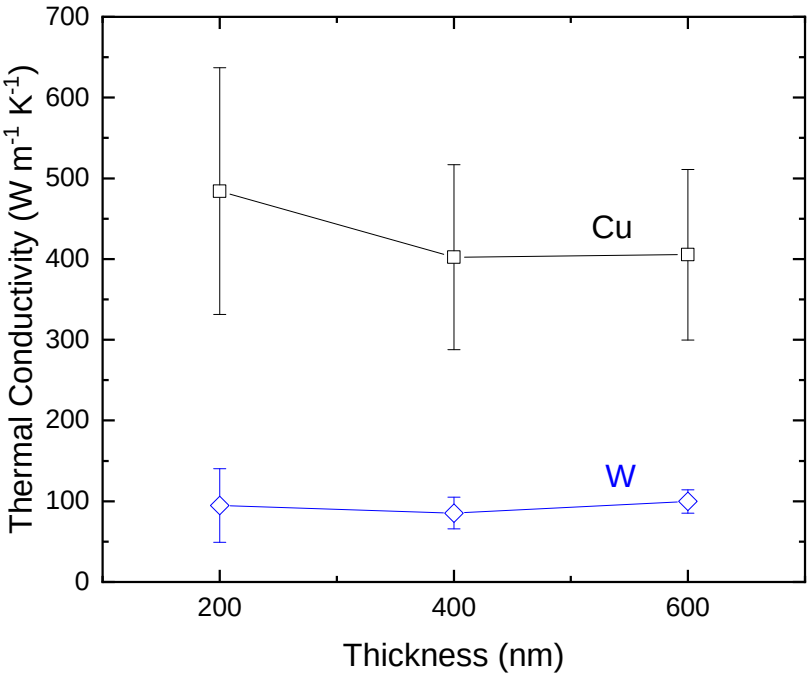

FIG. S8. Films of Cu and W were deposited upon Al_2O_3 wafers to provide reference thermal conductivities for the Cu and W buffer layers within the multilayer stacks. Film thicknesses ranged from 200 - 600 nm. The samples were coated with an 80 nm layer of Aluminum and measured with TDTR as described in the main manuscript. The TDTR data was analyzed as a three-layer model including the Al transducer, Cu or W film, and the Al_2O_3 substrates. the Thermal conductivity of the film as well as the thermal boundary conductance between the aluminum film were treated as fitting parameters. The backside thermal boundary conductance was assumed as 200 MW m^{-2} K^{-1}, which is typical for metal films on dielectric substrates.[22,23] For the highest film thickness of 600 nm, the Cu and W films have nominal thermal conductivities of 405 and 100 W m^{-1} K^{-1}, respectively. Within the literature, the thermal conductivity of bulk Cu and W are found to be on the order of 398[13] W m^{-1} $K^{-1}$and 178[24] W m^{-1} K^{-1}, respectively. The nominal fitted value of the Al/Cu interfaces ranged from 145 - 163 MW m^{-2} K^{-1} and 117 - 128 MW m^{-2} K^{-1} for Al/W. We observe high sensitivity to the thickness of Al transducer layer, and account for the standard deviation of the Al film thickness ($\pm$ 3 nm), as well as measurement repeatability in the uncertainty assessment of the measurements. While films within this thickness range do not display significant size effects, the W buffer layer used in the multilayer samples is 25 nm in nominal thickness, and as such we utilize a lower thermal conductivity of 52.2 W m^{-1} K^{-1}, taken from the literature,[21] for thin film W in the thermal model applied to the multilayer samples.

VI. NML LAYER PROPERTIES

TABLE S3. Layer properties for each of the NMLs. The labels correspond to the letters beside each sample plotted in Figure 5 of the main manuscript. d_{Cu} and d_{film} are the nominal film thicknesses of the copper and adjacent films within a given multilayer sample. d is the thickness of the overall sample. For the Cu/Ta and Cu/TaN multilayer materials, the thickness of the multilayer region was directly measured with XSEM; the nominal thickness was utilized in for the Cu/W multilayer samples as the thickness was much greater than the Cu/Ta or Cu/TaN samples. $\kappa_{measured}$ is the thermal conductivity of the multilayer region as measured through TDTR. $G_{Cu/film}$ is the mean thermal boundary conductance between the copper and adjacent films within the multilayer region, which was calculated for the Cu/W NMLs in the main manuscript.

NML	Fig. 5 label	d_{Cu} (nm)	d_{film} (nm)	d (nm)	$\kappa_{measured}$ (W m^{-1} K^{-1})	$G_{cu/film}$ (GW m^{-2} K^{-1})
Cu/Ta	a	5	5	238	8.8	-
	b	5	2	112.7	9.8	-
	c	5	5	117.9	8.9	-
	d	6	6	110.1	8.1	-
	e	8	8	117.9	8.6	-
	f	10	10	120.4	10.1	-
	g	20	20	120.4	10.7	-
Cu/TaN	a	5	2	118.5	8.5	-
	b	5	3.5	136	7.4	-
	c	5	5	115.6	7.0	-
	d	10	3.5	115.6	12.8	-
	e	5	5	253.5	6.3	-
Cu/W	a	3	3	600	11.3	4.1
	b	5	3	800	15.6	4.3
	c	10	3	1300	19.8	3.3
	d	10	5	1500	25.6	3.9
	e	5	5	1000	17.1	3.8

REFERENCES

[1]A. F. Mayadas, M. Shatzkes, and J. F. Janak, Appl. Phys. Lett. **14**, 345 (1969).

[2]J. S. Chawla, F. Gstrein, K. P. O'Brien, J. S. Clarke, and D. Gall, Phys. Rev. B **84**, 235423 (2011).

[3]C. Cancellieri, F. Moszner, M. Chiodi, S. Yoon, J. Janczak-Rusch, and L. P. H. Jeurgens, Journal of Applied Physics **120**, 195107 (2016), https://doi.org/10.1063/1.4967992.

[4]F. Moszner, C. Cancellieri, M. Chiodi, S. Yoon, D. Ariosa, J. Janczak-Rusch, and L. P. H. Jeurgens, Acta Mater. **107**, 345 (2016).

[5]B. C. Gundrum, D. G. Cahill, and R. S. Averback, Physical Review B - Condensed Matter and Materials Physics **72**, 245426 (2005).

[6]E. A. Scott, J. T. Gaskins, S. W. King, and P. E. Hopkins, APL Mater. **6**, 058302 (2018).

[7]Y. Touloukian and E. Buyco, *Thermophysical Properties of Matter—Specific Heat: Nonmetallic Solids, Vol. 5*, edited by Y. Touloukian and C. Ho (IFI/Plenum, New York, 1970).

[8]A. Sood, R. Cheaito, T. Bai, H. Kwon, Y. Wang, C. Li, L. Yates, T. Bougher, S. Graham, M. Asheghi, M. Goorsky, and K. E. Goodson, Nano Letters **18**, 3466 (2018).

[9]E. A. Scott, S. W. Smith, M. D. Henry, C. M. Rost, A. Giri, J. T. Gaskins, S. S. Fields, S. T. Jaszewski, J. F. Ihlefeld, and P. E. Hopkins, Applied Physics Letters **113** (2018), 10.1063/1.5052244.

[10]P. E. Hopkins, L. M. Phinney, J. R. Serrano, and T. E. Beechem, Physical Review B - Condensed Matter and Materials Physics **82**, 085307 (2010).

[11]W. F. Giauque and P. F. Meads, Journal of the American Chemical Society **63**, 1897 (1941).

[12]P. Nath and K. Chopra, Thin Solid Films **20**, 53 (1974).

[13]A. Tesfamicha and A. D. Woldeyo, Asian Journal of Scientific Research **6**, 339 (2013).

[14]J. Bryner, D. M. Profunser, J. Vollmann, E. Mueller, and J. Dual, Ultrasonics **44**, e1269 (2006).

[15]E. Bozorg-Grayeli, Z. Li, M. Asheghi, G. Delgado, A. Pokrovsky, M. Panzer, D. Wack, and K. E. Goodson, Applied Physics Letters **99**, 261906 (2011).

[16]C. H. Mastrangelo, T. Yu-Chong, and R. S. Muller, Sensors and Actuators A: Physical **23**, 856 (1990).

[17]N. Stojanovic, J. Yun, J. M. Berg, M. Holtz, and H. Temkin, **16**, 639 (2009).

[18]J. T. Gaskins, P. E. Hopkins, D. R. Merrill, S. R. Bauers, E. Hadland, D. C. Johnson, D. Koh, J. H. Yum, S. Banerjee, B. J. Nordell, M. M. Paquette, A. N. Caruso, W. A. Lanford, P. Henry,

L. Ross, H. Li, L. Li, M. French, A. M. Rudolph, and S. W. King, ECS Journal of Solid State Science and Technology **6**, N189 (2017).

[19]J. L. Braun, D. H. Olson, J. T. Gaskins, and P. E. Hopkins, Review of Scientific Instruments **90** (2019), 10.1063/1.5056182.

[20]G. White and S. Collocott, Journal of Physical and Chemical Reference Data **13**, 1251 (1984).

[21]J. Hostetler, A. Smith, and P. Norris, Microscale Thermophysical Engineering **1**, 237 (1997).

[22]R. Cheaito, J. T. Gaskins, M. E. Caplan, B. F. Donovan, B. M. Foley, A. Giri, J. C. Duda, C. J. Szwejkowski, C. Constantin, H. J. Brown-Shaklee, J. F. Ihlefeld, and P. E. Hopkins, Phys. Rev. B **91**, 035432 (2015).

[23]P. E. Hopkins, ISRN Mechanical Engineering **2013** (2013), 10.1155/2013/682586.

[24]R. Powell, C. Y. Ho, and P. E. Liley, *Thermal conductivity of selected materials*, Vol. 8 (US Department of Commerce, National Bureau of Standards Washington, DC, 1966).